



# Temporal Variation of Charring Depth of the Wood-Frame Walls in Fire

Shu-Fen Tung<sup>1</sup>, Hung-Chi Su<sup>1</sup>, C. T. Tzeng<sup>1</sup>, Yi-Pin Lin<sup>2</sup>, and Chi-Ming Lai<sup>3</sup>(✉)

<sup>1</sup> Department of Architecture, National Cheng Kung University, Tainan City, Taiwan

<sup>2</sup> Department of Creative Design, National Yunlin University of Science and Technology, Douliu City, Taiwan

<sup>3</sup> Department of Civil Engineering, National Cheng Kung University, Tainan City, Taiwan  
cmlai@mail.ncku.edu.tw

**Abstract.** In this study, temporal variation of charring depth of wood studs inside wood-frame walls (WFWs) in fire was investigated. First, the time variation in the surface temperature of wood studs inside WFWs was determined based on ISO 834 fire-resistance tests, and the resulting heating conditions were used in subsequent heat exposure tests. Then, wood stud specimens of four different wood species (Chinese fir, Japanese cedar, southern pine and spruce) were each subjected to a heat exposure test in an electric furnace. The results exhibited no significant correlation between the charring depth of the wood stud specimens and the pre-heating density. In addition, the test data validated that the equation proposed by Sugahara can be used for predicting the charring depth of wood studs inside WFWs in a fire.

**Keywords:** Fire · Char · Wood-frame wall · Stud · Wood

## 1 Introduction

Wood-frame walls (WFWs) commonly seen in practice, consist of wood studs, covering panels, insulation materials in joist and stud cavities, and fasteners. The constituent parts with standardized sizes and modules are fabricated in factories and assembled at construction sites to save material, construction costs and promote construction quality. For WFWs, fire resistance is critical and important due to the reduction of the cross-sections of wood studs and the strength and stiffness of the heated zone when exposed to fire [1]. To evaluate the fire resistance of WFWs, it is therefore necessary to predict the thermal degradation (charring) of wood studs.

Wood charring studies can be classified into several types based on the fire source [2]: (1) those in which the specimen is heated with a heat flux generated at the specimen boundary using a cone calorimeter or other bench-scale tests, (2) those in which the specimen is heated in an ASTM E 119 or ISO 834 fire endurance test furnace using the provided time-temperature variation curve, and (3) those in which the charring of wood is observed in room (or multi-room) fire or a building fire.

Using cone calorimeter tests, Xu et al. [3] examined the charring properties of five common timber species, three of which were softwood species (Douglas fir (*Pseudotsuga*

*menziesii*), Scots pine (*Pinus sylvestris*) and Southern pine (genus *Pinus*) and two of which were hardwood species (Shorea (a species of the genus *Dipterocarpaceae*) and merbau (*Intsia bijuga*)). It found that except for the merbau specimens, the equations recommended by the European Committee for Standardization (Eurocode 5, EC) and the Australian Standard (AS 1720.4) both underestimated the charring depth of the specimens.

In this study, to determine the variation in the charring depth of wood studs in WFWs when exposed to a fire, wood stud specimens made of four wood species were each subjected to a heat exposure test under varying temperature conditions, which were set based on the ISO 834 fire-resistance test results for WFWs. Detailed information on this study can be found in [4].

## 2 Research Method

### 2.1 Preliminary Test Specimens and Heating Conditions

In this study, the transient temperature distribution in wood studs in WFWs was determined by fire-resistance tests, which were used as the heating conditions for the subsequent principal test. During the fire-resistance tests, the heating conditions inside the furnace were set based on the heating curves specified in the ISO 834-1 (1999): Fire-resistance tests – Elements of building construction – Part 1: General requirements and the ISO 834-8 (2002): Fire-resistance tests – Elements of building construction – Part 8: Specific requirements for non-load bearing vertical separating elements. The specimens were heated for 60 min. Four full-scale WFW specimens of various sizes were prepared with two types of covering boards (gypsum and calcium silicate boards) and studs of two sizes (38 × 89 mm and 38 × 140 mm). Figure 1 shows the specimens and the locations of thermocouples (marked ① and ②). Table 1 shows the structural details of the WFW specimens. Figure 2 shows the ISO 834 furnace used in this study. The device is located in the Fire Experiment Center, Architecture & Building Research Institute, Ministry of Interior, on the Gueiren Campus of National Cheng Kung University, Taiwan.

As shown in Table 2, the temperatures measured at locations ① and ② (see Fig. 1 for the measurement point locations) on specimens A and C shown in Table 1 were averaged and used as the temperature condition for the CFS (S indicates silicate boards) fire scenario. Specimens A and C were made of the same surface material (silicate boards) but differed in wood stud size (the stud section depths were 89 and 140 mm for specimens A and C, respectively). Similarly, the temperatures measured at locations ① and ② (see Fig. 1 for the measurement point locations) on specimens B and D shown in Table 1 were averaged and used as the temperature condition for the CFG (G indicates gypsum boards) fire scenario. The surface heating curves of the wood studs tested in the CFS and CFG fire scenarios, as shown in Fig. 3, were used as the thermal boundary conditions for the subsequent principal test and the estimation of the charring depth.

## 3 Tested Wood Studs and Heat Exposure Experiments

Wood stud specimens made of four common wood species used to produce wood studs, namely, Chinese fir (*Cunninghamia lanceolata*), Japanese cedar (*Cryptomeria japonica*), Southern pine (*Pinus* spp.) and spruce, were selected as principal test specimens. After

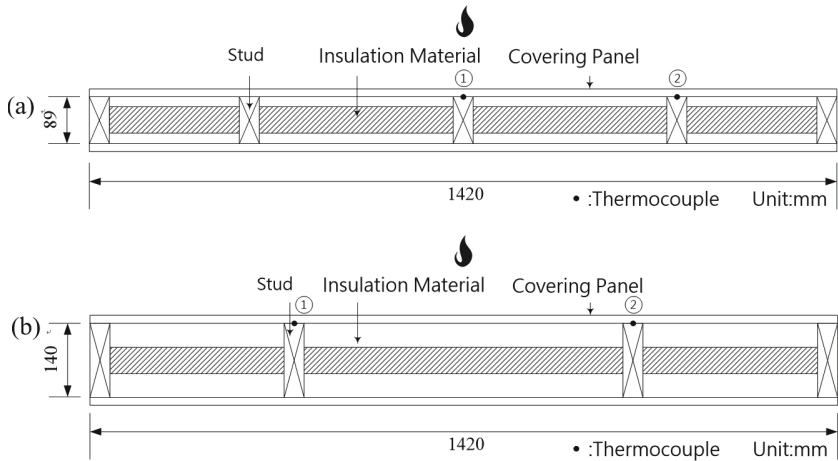


**Fig. 1.** WFWs and the positions of thermocouples for the pretests ((a): specimens A and D in Table 1; (b): specimens B and C in Table 1).



**Fig. 2.** ISO 834 Furnace used in this study.

being dried, these specimens each had moisture content below 19%. In addition, these specimens were trimmed to achieve a cross-sectional dimension of  $14 \times 14$  cm. The Chinese fir, Japanese cedar, southern pine and spruce specimens had an average density of  $448 \text{ kg m}^{-3}$ ,  $525 \text{ kg m}^{-3}$ ,  $681 \text{ kg m}^{-3}$  and  $551 \text{ kg m}^{-3}$ , respectively.

These specimens were each subjected to a heat exposure test in an electric furnace to simulate their conditions when exposed to a fire. Inside the furnace, a heater was placed on each of the top, left and right sides. The two ends and bottom of each specimen were covered with a heat insulator, thereby allowing the other three sides (top and two

**Table 1.** Details of the pretest specimens.

Specimen No	A	B	C	D
Species of the stud	Spruce (SPF)	Spruce (SPF)	Spruce (SPF)	Spruce (SPF)
Section of the stud	38 × 89 mm	38 × 140 mm	38 × 140 mm	(38 × 89 mm)
Covering panel	12 mm Silicate board	15 mm Gypsum board	12 mm Silicate board	15 mm Gypsum board
Insulation material	Mineral wool	Mineral wool	Mineral wool	Mineral wool

**Table 2.** Temperature calculation for the CFS and CFG fire scenarios.

Fire scenario	Temperature calculation	Time to reach 300 °C	Max. Temperature
CFS	<sup>a</sup> (A1 + A2 + C1 + C2)/4	19 min 50 s	702.5 °C
CFG	<sup>b</sup> (B1 + B2 + D1 + D2)/4	27 min 20 s	756.0 °C

<sup>a</sup>The average temperature measured by thermocouples embedded at positions 1 and 2 of specimen A and those of specimen C (see Table 1 for A and C). <sup>b</sup>The average temperature measured by thermocouples embedded at positions 1 and 2 of specimen B and those of specimen D

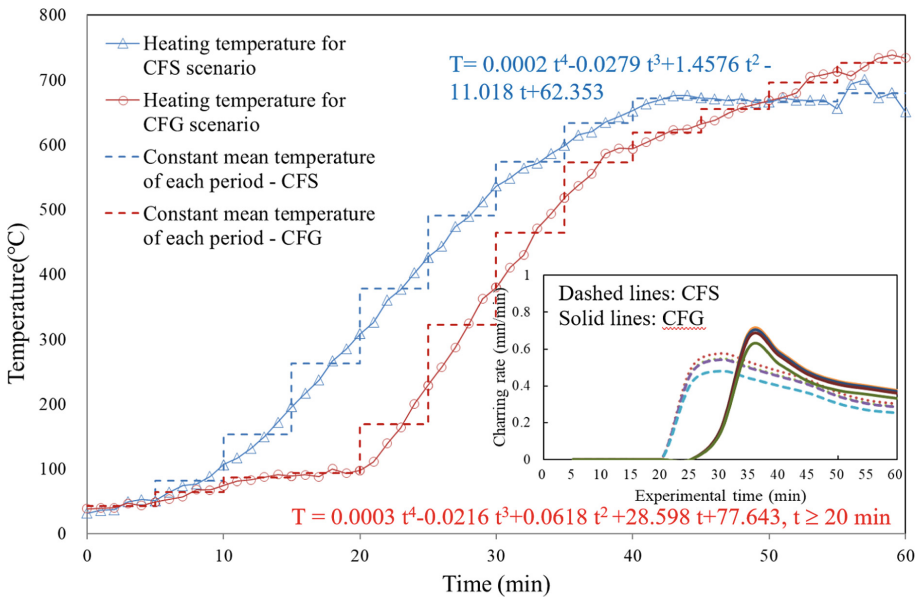


**Fig. 3.** The time–temperature curves and charring rate variations in the CFS and CFG fire scenarios for follow-up heat exposure experiments.

lateral sides) to be heated evenly to simulate damage on three sides caused by a fire (i.e., after the covering plate fell off as a result of fire exposure (post-protection phase)).

The air temperature inside the furnace was automatically increased based on Fig. 3 and recorded.

#### 4 Prediction of the Charring Depth of the Wood Stud Specimens

The charring depth of the wood stud specimens was predicted by substituting the principal test conditions (Fig. 3) into the correlation equations proposed by Hamada (1953) [5] and Sugahara (1978) [6] (hereinafter, the Hamada equation and the Sugahara equation). The predicted value of the charring depth of each specimen at 60 min was compared with the measured value. Equation (1) shows the Hamada equation for predicting the charring depth of wood under isothermal heating boundary conditions:

$$x = a \left( \frac{T}{100} - 2.5 \right) \sqrt{t} \quad (1)$$

where:

- x - charring depth (mm),
- t - heat exposure time (min),
- T - heating temperature ( $^{\circ}\text{C}$ ),
- a - the constant with a value that depends on the wood type.

Equation (2) shows the Sugahara equation for predicting the charring depth of wood under convective heating boundary conditions:

$$\begin{aligned} T &= (T_f - T_a) \operatorname{erf}(\eta) + T_a \\ &= \frac{X}{2\sqrt{\alpha t}}, X = x + d, d = \frac{k}{h}, \alpha = \frac{k}{\rho C} \end{aligned} \quad (2)$$

where:

- T - temperature of the charring front ( $^{\circ}\text{C}$ ),
- $T_f$  - ambient temperature ( $^{\circ}\text{C}$ ),
- $T_a$  - initial temperature ( $^{\circ}\text{C}$ ),
- $\operatorname{erf}(\eta)$  - complementary error function,
- $\eta$  - similarity variable,
- x - charring depth (mm),
- k - thermal conductivity ( $\text{kcal} \cdot \text{m}^{-1} \text{h}^{-1} \text{C}^{-1}$ ),
- h - convective heat transfer coefficient ( $\text{kcal} \cdot \text{m}^{-2} \text{h}^{-1} \text{C}^{-1}$ ),
- $\rho$  - the density ( $\text{kg} \cdot \text{m}^{-3}$ ),
- C - specific heat capacity ( $\text{kcal} \cdot \text{kg}^{-1} \text{C}^{-1}$ ).

The charring depth of the wood stud specimens was estimated based on the above equations in conjunction with the standard heating curves proposed in this study (Fig. 3) using the following procedure:

1. Each time-temperature curve used to control the heating process was divided into several time segments, as shown in Fig. 3. The average temperature in each time segment was determined by averaging the corresponding heating temperatures.

2. The average charring rate and charring depth in a certain time segment were calculated using the Hamada and Sugahara equations, respectively, as shown in Fig. 4.
3. Based on the start time of charring defined in the previously mentioned step and the aforementioned time and location, the cumulative charring depth within a certain time segment was determined.
4. The variation in the charring depth of each wood stud specimen with time was then determined based on the sum of the charring depths in all the time segments.

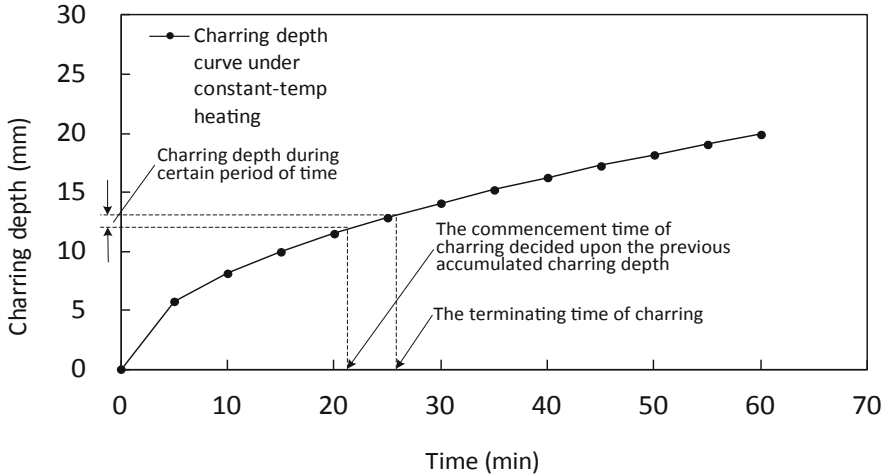


**Fig. 4.** Method of calculating the charring depth used in this study

## 5 Results and Discussion

Figure 5 shows a comparison of the predicted values of the charring depth of each specimen obtained using the Hamada [5] and Sugahara [6] equations (Eqs. 1 and 2, respectively) and the measured values. As demonstrated in Fig. 8, the predicted values obtained using the Hamada equation differed considerably from the measured values, whereas the predicted values obtained using the Sugahara equation were in good agreement with the measured values.

The predicted values obtained using the Sugahara equations were relatively close to the measured values (average  $r$ : 0.83). In addition to density, the Sugahara equation contains the coefficient of heat convection. Because the accounts for the convection of hot air resulting from a fire, the Sugahara equation aligns with the use of an actual fire as thermal boundary conditions in this study. As a result, the predicted values obtained using the Sugahara equations were very close to the measured values.

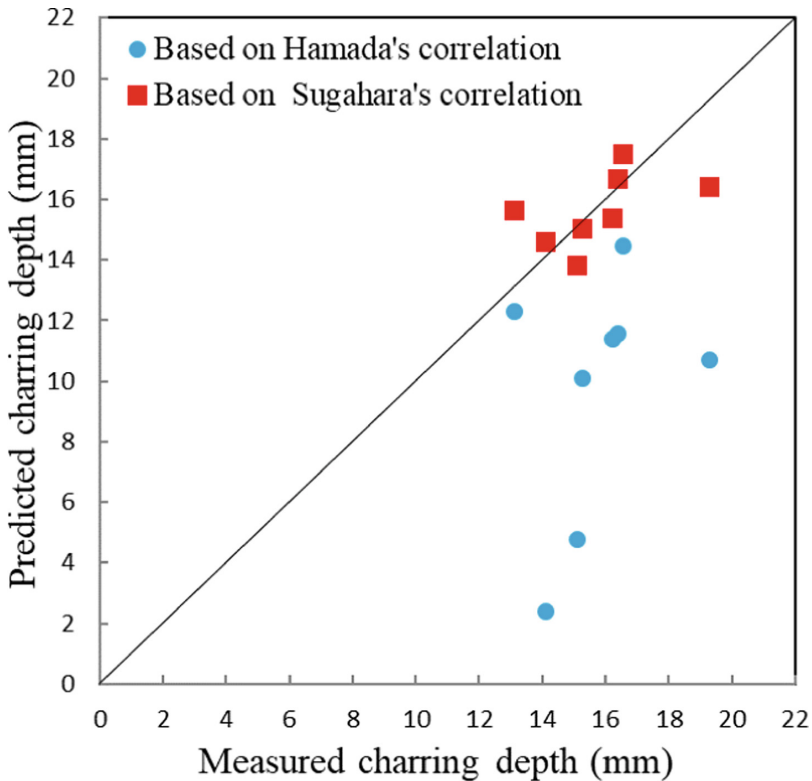


**Fig. 5.** The relationship between the experimental and predicted charring depths of four wood species (China fir, Japanese cedar, Southern pine and spruce)

## 6 Conclusion

1. For the predicted values of the charring depth obtained using the Hamada equation, only those of the wood stud specimens with densities in the range of  $0.35 \text{ g}\cdot\text{cm}^{-3}$ – $0.5 \text{ g}\cdot\text{cm}^{-3}$  were relatively close to the measured values.
2. For the predicted values of the charring depth obtained using the Sugahara equation (Fig. 3), those of the wood stud specimens with densities in the range of  $0.4 \text{ g}\cdot\text{cm}^{-3}$ – $0.72 \text{ g}\cdot\text{cm}^{-3}$  were very close to the measured values. Thus, Sugahara equation is recommended to be used to predict the charring depth of woods studs inside WFWs in a fire.

## References

1. Östman, B., Brandon, D., Frantzych, H.: Fire safety engineering in timber buildings. *Fire Saf. J.* **91**, 11–20 (2017)
2. Babrauskas, V.: Charring rate of wood as a tool for fire investigation. *Fire Saf. J.* **40**(6), 528–554 (2005)

3. Xu, Q., Chen, L., Harries, K.A., Zhang, F., Liu, Q., Feng, J.: Combustion and charring properties of five common constructional wood species from cone calorimeter tests. *Constr. Build. Mater.* **96**, 416–427 (2015)
4. Su, H.C., Tung, S.F., Tzeng, C.T., Lai, C.M.: Variation in the charring depth of wood studs inside wood-frame walls with time in a fire. *Wood Res.* **64**(3), 449–460 (2019)
5. Hamada, M.: Wood burning rate. *Proc. Jpn. Soc. Fire* **2**, 106–107 (1953)
6. Sugahara, S.: Study of wood carbonization rate. Summaries of technical papers of annual meeting, *Archit. Inst. Jpn.*: 2109–2110 (1978)